nature communications

Article

https://doi.org/10.1038/s41467-025-65015-4

A rapidly closing window for coral persistence under global warming

Received: 22 January 2025

Accepted: 3 October 2025

Published online: 05 November 2025

Check for updates

Yves-Marie Bozec[1] ✉, Arne A. S. Adam[1], Beatriz Arellano-Nava[2], Anna K. Cresswell[3,4], Vanessa Haller-Bull[3], Takuya Iwanaga[3], Liam Lachs[5], Samuel A. Matthews[3], Jennifer K. McWhorter[6], Kenneth R. N. Anthony[3,7], Scott A. Condie[8], Paul R. Halloran[2], Juan-Carlos Ortiz[3], Cynthia Riginos[1,3] & Peter J. Mumby[1]

Coral reefs around the world are increasingly threatened by marine heatwaves causing widespread coral bleaching and mortality. Global analyses of projected heatwaves can inform decision-making, but forecasting the interactions between disturbance refugia, coral life histories and capacity to adapt is key for guiding strategic management of coral persistence. Here, we simulate coral eco-evolutionary dynamics across 3800 reefs of Australia's Great Barrier Reef under current climate projections. We project a rapid coral decline by mid-century under all emission scenarios, with further decline under the most likely warming trajectory. However, recovery is possible this century if warming remains below 2 °C, allowing thermal adaptation to keep pace. Our simulations show that resilient reefs are primarily in bleaching refugia, which also support a greater diversity of thermal phenotypes. While cool-adapted corals disperse to warm spots, we found no evidence of 'gene swamping' undermining thermal adaptation. Our findings highlight that management opportunities exist to promote adaptation in thermal refugia and warm spots, but emphasize that curbing global warming by 2050 is crucial for coral persistence.

Anthropogenic greenhouse-gas (GHG) emissions have raised global temperatures by roughly 1 °C above pre-industrial levels[1], intensifying the frequency and severity of marine heatwaves and driving tropical coral reef ecosystems into decline[2–5]. Heat stress disrupts the symbiotic relationship between reef-building corals and their photosynthetic algal endosymbionts (zooxanthellae), leading to coral bleaching[6]. Under severe and prolonged heat stress, persistent coral bleaching leads to extensive mortality[4–7]. Regional-scale marine heatwaves are occurring at an alarming rate, significantly reducing the recovery time between consecutive bleaching events[2,8,9]. This poses an unprecedented threat to the persistence of functioning coral reef ecosystems in the twenty-first century: even with the most aggressive reduction of GHG emissions, global warming is expected to exceed 1.5 °C for multiple decades[10].

Mitigating future warming impacts on coral reefs requires strategic management that adopts a long-term lens[11,12]. Projections of reef futures have focused almost entirely on evaluating the likelihood that temperatures will exceed current thresholds for widespread coral mortality[13–15]. These projections fail to account for evolutionary processes and the adaptive capacity of corals, the diversity of coral life-

[1]School of the Environment, University of Queensland, St Lucia, QLD, Australia. [2]Global Systems Institute and Geography Department, University of Exeter, Exeter, UK. [3]Australian Institute of Marine Science, Townsville, QLD, Australia. [4]Oceans Institute, University of Western Australia, Perth, WA, Australia. [5]School of Natural and Environmental Sciences, Newcastle University, Newcastle upon Tyne, UK. [6]Cooperative Institute for Marine and Atmospheric Studies, Rosenstiel School of Marine, Atmospheric, and Earth Science, University of Miami, Miami, FL, USA. [7]Queensland University of Technology, Gardens Point, Brisbane, QLD, Australia. [8]CSIRO Environment, Hobart, TAS, Australia. ✉e-mail: y.bozec@uq.edu.au

histories, and the complex demographics of interconnected coral metacommunities within a spatially heterogeneous environment, including disturbance refugia[16]. The ability of corals to withstand rising sea temperatures will partly depend on their adaptive potential (i.e., evolutionary rescue[17]), yet the degree to which natural selection can enhance heat tolerance under frequent and intense marine heatwaves is unknown. Population persistence might also be promoted by coral larvae supplied by nearby reef habitats (i.e., demographic rescue[18]), but the resilience of larval dispersal networks remains uncertain given the large geographic footprint of marine heatwaves[19]. The fate of coral reefs will ultimately hinge on how effectively these rescue effects may combine to enhance resistance to bleaching and support recovery, which in turn will be influenced heavily by the rate of temperature change in the next decades.

Here, we explore the eco-evolutionary response of coral communities to climate change using a comprehensive and field-tested ecosystem model of Australia's iconic Great Barrier Reef[20], extended to include adaptive evolution to thermal stress. By simulating community evolutionary dynamics throughout the twenty-first century, we evaluate coral persistence under alternative scenarios of GHG emissions and assess the potential for rapid coral evolution across multiple spatial and temporal scales. While our findings paint a grim future for coral reefs, we do identify paths under which coral populations may adapt and persist. We also find opportunities for management interventions to capitalise on coral connectivity patterns and anticipated future warming (thermal refugia and warm spots) for supporting reef resilience, reinforcing the value of taking a strategic and proactive approach to managing climate change impacts.

Results

Modelling coral eco-evolutionary dynamics

Our model, ReefMod-GBR[20], simulates individual corals recruiting, growing, competing, reproducing and dying on 3806 individual reefs interconnected by larval dispersal along the ~2300 km length of the Great Barrier Reef (Fig. 1a). Each modelled reef is subject to a specific environmental setting, including water quality, larval connectivity, outbreaks of the coral-eating starfish (*Acanthaster* spp.) and the incidence of cyclones and marine heatwaves. Corals are classified into six groups with variable demographics and susceptibility to disturbances. Temperature-induced mortality (Fig. 1b) is estimated from the Degree Heating Week (DHW; °C-week), a measure of accumulated heat stress exposure[4,21] proven to be a reliable proxy for coral bleaching and mortality on the Great Barrier Reef[5]. Sensitivity to heat stress is a quantitative trait modelled at the level of individual coral colonies, capturing variations in heat tolerance within[22] (Fig. 1b, c) and among coral groups[5,20] (Supplementary Fig. 2c). Heat tolerance is partially inherited[23], with a heritability coefficient that aligns with empirical estimates for coral thermal traits[24,25]. Incorporating individual-level variations and the heritability of heat tolerance enables thermal adaptation across multiple generations. This adaptive process is driven by natural selection in response to successive mass bleaching and mortality events, promoting the survival and propagation of thermally-tolerant phenotypes.

We begin by simulating coral community dynamics of the past 15 years to capture the recent selective pressures experienced across the Great Barrier Reef—a cluster of four significant marine heatwaves that occurred in 2016, 2017, 2020 and 2022 (Supplementary Fig. 4a). Starting in 2008 from an average 27.4% coral cover (95% prediction interval: 27.2–27.7%) informed by historical monitoring, simulations reveal large temporal fluctuations across the 3806 reefs (Supplementary Fig. 5), underscoring both periods of substantial coral declines and periods of remarkable recovery. The model predicts an average coral cover of 38.8% in 2023 (38.1–39.4%), reflecting an overall increase from 2008. However, the hindcast reveals prolonged periods of low coral cover as indicated by a 25.4% annual average (13.8–37.1%). The comparison with monitoring data indicates a credible reconstruction of the past trajectory of mean coral cover (Supplementary Fig. 5), with model errors—defined as the annual differences between predictions and observations—being evenly distributed over time (Supplementary Fig. 6) and having a mean value of −0.3 percentage points (95% central interval: −9.3–7.5%). Coral cover reconstructions at individual-reef scales performed reasonably well (Supplementary Fig. 7), with model errors primarily arising from the difficulty of hindcasting patchy disturbances at fine resolution, especially the damaging waves generated by cyclones[20,26,27]. However, these discrepancies reflect the accuracy of the hindcast only and do not constrain future uncertainty, provided it is captured by stochastic disturbance scenarios and the model's representation of coral responses to specified disturbance intensities.

The modelling of coral bleaching, parameterised with in situ mortality data from the 2016 marine heatwave[5,20], allows for an accurate reconstruction of relative coral cover changes observed from independent monitoring[28] (Fig. 1d). Simulated demographics before and after heat stress predict, on average, a 38% coral decline (15–60%) to DHW exposures between 8–10 °C-week, resulting in an average shift of +1.6 °C-week (1.1–2.2 °C-week) in the mean heat tolerance of thermally-sensitive taxa (Fig. 1e). Reliable predictions of coral bleaching responses were also obtained in 2017 and 2022, but not in 2020, as no significant mortality was reported despite reef exposure to harmful DHW levels (Supplementary Fig. 8). As the modelled coral communities were assumed to be relatively naive to heat stress prior to the 2016 mass bleaching, coral mortality decreased during the subsequent bleaching events in 2017, 2020 and 2022, with a mean coral decline of, respectively, 28% (0–57%), 28% (5–52%) and 10% (0–29%) on reefs exposed to 8–10 °C-week. Hence, the response to bleaching weakens across successive marine heatwaves due to the progressive elimination of the most thermally-sensitive corals (Supplementary Fig. 9). The strength and persistence of this shift in heat tolerance depend on the intensity of the selective pressure, the rate at which new corals recruit, their thermal traits, and the effective transmission of these traits to subsequent generations.

Projected heat stress under different warming scenarios

We used daily projections of sea surface temperatures (SST) derived from the Coupled Model Intercomparison Project Phase 6 (CMIP6)[29] to simulate the impacts of future bleaching events under five alternative GHG emissions scenarios (Shared Socioeconomic Pathway, SSP) assessed in the latest IPCC report[10]. Daily SST projections of ten climate models were downscaled to 10 km using semi-dynamical shelf-sea modelling[30], allowing us to calculate annual maximum DHW for each individual reef from 2024 to 2100.

Our DHW projections reveal an escalation in the frequency and intensity of marine heatwaves in the coming decades under all emission scenarios (Fig. 2a). Only rapid and drastic reductions of GHG emissions, limiting global warming to +1.5 °C (SSP1-1.9), have the potential to reduce SST in the latter half of the century. Adhering to the +2 °C limit set by the 2015 Paris Agreement (SSP1-2.6) would only stabilise SST by the end of the century, yet restricting global warming below 2 °C requires immediate and strong mitigation actions[31,32]. Under a more likely scenario of ~2.7 °C global warming[33,34] (SSP2-4.5), SST will continue to rise after mid-century, exposing 50% of the Great Barrier Reef to DHW above 8 °C-week (a threshold of widespread bleaching and mortality in heat-sensitive corals[4,35]) at a rate greater than 5 events per decade (Supplementary Fig. 10). Note there is important spatial heterogeneity in the frequency of heat stress, with 10% of reefs expected to experience DHW > 8 °C-week only 1–4 times per decade, while 10% would experience it almost annually. Heat stress above 16 °C-week, conducive of severe multi-species coral mortality[36], would affect 50% of the reefs at a rate greater than 3 events per decade. Under more severe warming scenarios (SSP3-7.0: ~3.6 °C; SSP5-8.5: ~4.4 °C; ref. 1), heat stress above 16 °C-week is projected to affect more than 50% of the Great Barrier Reef at a frequency greater than 6 events per decade after 2060, and annually by 2100.

https://doi.org/10.1038/s41467-025-65015-4

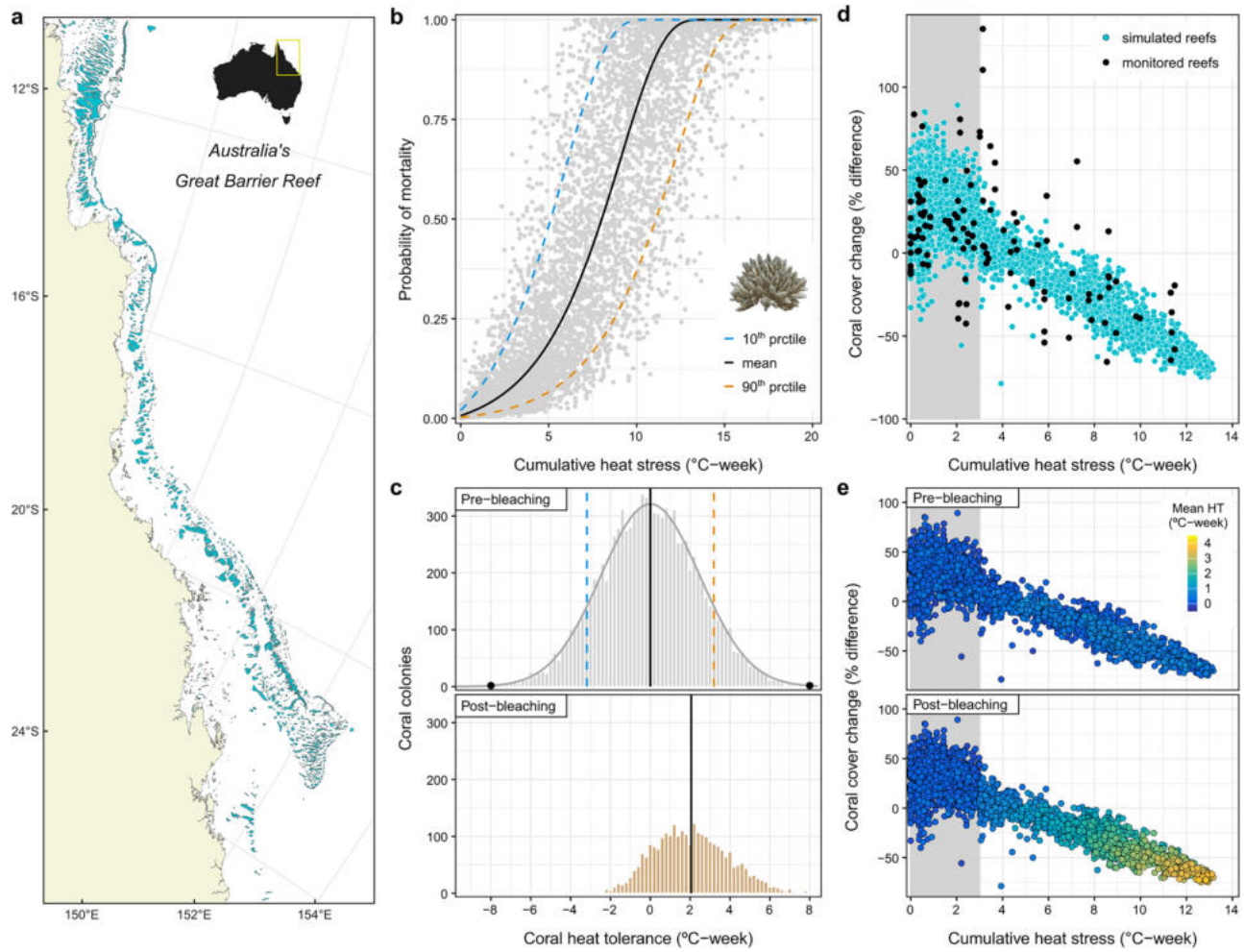

Fig. 1 | Modelling of coral eco-evolutionary dynamics. a Spatial domain of ReefMod-GBR, consisting in $n = 3806$ individual reef units (blue polygons) distributed along Australia's Great Barrier Reef (GBR). Reef polygons were mapped using the Great Barrier Reef Marine Park Authority geospatial data 'Great Barrier Reef Features (GDA94)' under licence CC BY 4.0. Australia map (inset) from Wikimedia Commons under licence CC BY-SA 3.0, https://commons.wikimedia.org/wiki/File:Australia_Locator_Map_(alt).svg. **b** Bleaching-induced coral mortality resulting from accumulated heat stress (Degree Heating Week, DHW, in °C-week) at initialisation (i.e., naive response to heat stress). Corals of a given group (here, corymbose acroporids) follow an average dose-response (black curve) modelled from depth-adjusted mortality observed during the 2016 mass bleaching[5,20]. Variability in heat tolerance (±HT; °C-week) among coral individuals (grey dots, $n = 10{,}000$ randomly generated) is simulated by shifting the dose-response curve horizontally along the DHW axis, reflecting individual deviations from the group mean response at initialisation. The blue and orange mortality curves (dashed lines) indicate, respectively, the bleaching response of the 10th and 90th percentiles of the HT distribution within the group[22]. Coral image courtesy of C. Castro-Sanguino. **c** Simulated HT distributions before ($n = 10{,}000$ colonies) and after ($n = 2693$ colonies) a hypothetical heat stress of 10 °C-week, illustrating the natural selection of heat-tolerant corals. At initialisation, the distribution is truncated normal, with mean 0 °C-week (black line), the 10th and 90th percentiles as in (**b**), and limits set to ± 8 °C-week (black dots). **d** Impacts of the 2016 mass bleaching on total coral cover (relative change) recorded at 5–10 m depth by independent monitoring surveys[28] (black dots, $n = 117$ reefs) and predicted by the model (blue dots, $n = 3806$ reefs), versus reef-level DHW exposure recorded by remote sensing[21]. In the model, bleaching does not occur when reefs are exposed to 0–3 °C-week (grey area) following ref. 5. **e** Simulated 2016 bleaching impacts on total coral cover ($n = 3806$ reefs) as in (**d**), showing changes in the mean tolerance of heat-sensitive coral groups (acroporids and pocilloporids) following selection by bleaching.

By comparison, the recent marine heatwaves have exposed 20–30% of the Great Barrier Reef to more than 8 °C-week with a maximum of 13.3 °C-week (Supplementary Fig. 4a), although only a few reefs were affected by all four events[37]. However, we note that our downscaled ensemble climate model, with SST projections starting effectively in 2014, hindcasts more extreme DHWs than those actually observed (Supplementary Fig. 4b). This discrepancy may reveal a warm bias in our SST projections, potentially overestimating future heat stress events in the early years of climate forecasting.

Future coral cover trajectories

Predicting the precise timing, location and intensity of acute disturbances is impossible. However, using an ensemble of stochastic simulations of marine heatwaves and tropical cyclones, we can project an array of feasible futures to understand differences in reef dynamics under alternative emissions scenarios. Since some CMIP6 climate models are more sensitive than others to anthropogenic climate forcing[38,39], we designed an ensemble approach that weights climate models based on the likelihood of their equilibrium climate sensitivity (the increase in global temperature resulting from a doubling of atmospheric CO_2, Supplementary Fig. 11). We assess coral projections based on the 'likely' distributions of the average coral cover across the Great Barrier Reef derived annually from the CMIP6 weighted ensemble of climate forecasts.

Our eco-evolutionary simulations project a sharp coral decline over the next 15 years for all emission scenarios (Fig. 2b), with mean coral cover dropping to 17% in 2040 (mean of the likely distribution across all SSPs, 95% prediction interval: 0–39%). This corresponds to a

https://doi.org/10.1038/s41467-025-65015-4

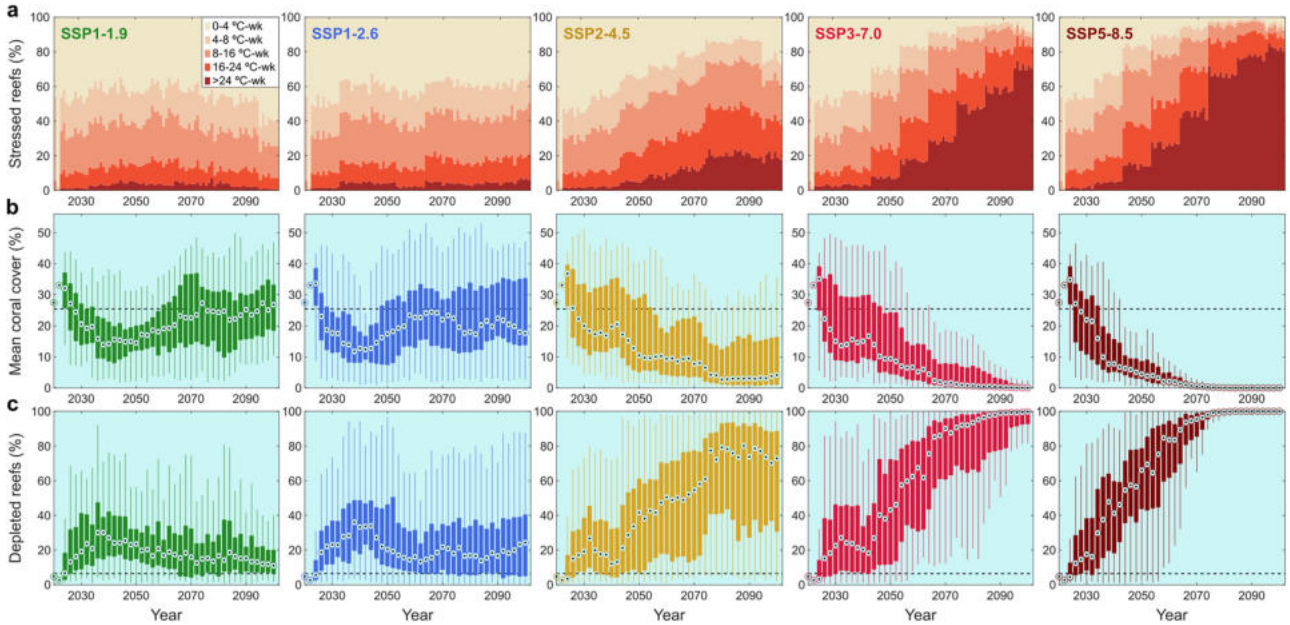

Fig. 2 | Ensemble projections of Australia's Great Barrier Reef during the twenty-first century under five climate futures. From left to right, projections are shown for five scenarios of socioeconomic development (Shared Socioeconomic Pathways, SSPs), SSP1-1.9, SSP1-2.6, SSP2-4.5, SSP3-7.0, and SSP5-8.5, leading to a global warming by 2100 of (best estimate[1]) +1.4 °C, +1.8 °C, +2.7 °C, +3.6 °C and +4.4 °C, respectively. **a** Percentage of reefs ($n = 3806$) under different categories of heat stress (Degree heating Weeks, DHW) across all climate projections ($n = 140$ projections for SSP1-1.9, $n = 200$ for all other SSPs). DHW events within each downscaled climate projection were shuffled per decade to generate stochastic fluctuations in the occurrence of bleaching. **b** Likely biennial distributions of the predicted Great Barrier Reef mean total coral cover (percent cover of all corals averaged across all reefs) among 1000 bootstrap samples, each consisting of 20 individual runs of the eco-evolutionary model drawn at random using the likelihood of the underlying climate projection as weight. Boxes represent the interquartile range (IQR), showing the spread of mean total coral cover predictions between the 25th (Q1) and 75th percentiles (Q3) of the likely distributions ($n = 20{,}000$ predictions for each biennial distribution). Whiskers extend from each box to the most extreme samples not considered outliers. Outliers (not shown for clarity) are samples greater than $Q3 + 1.5 \times IQR$ or less than $Q1 - 1.5 \times IQR$. The central point mark is the median. **c** Distribution of the proportion of reefs with total coral cover <5%. Boxes, whiskers and central point as for (**b**). In **b** and **c**, the dashed lines indicate the hindcast (2008–2023) averages for reference (25.4% total coral cover, 6.5% of reefs in a depleted state).

56% decline of the present-day mean coral cover. Keeping global warming below 2 °C (SSP1-1.9: ~1.4 °C; SSP1-2.6: ~1.8 °C; ref. 1) would promote coral recovery in the second half of the century as SST ceases to rise, though retrieving the contemporary levels of coral cover would require the most stringent mitigation of GHG emissions (SSP1-1.9). Under a more likely global warming of ~2.7 °C (SSP2-4.5), coral populations would decline throughout the century, with projections of mean coral cover dropping to 16% (0–40%) by 2050 and 8% (0–26%) by 2100. By the end of the century, the vast majority of individual reefs (>60%) would be depleted to less than 5% total coral cover (Fig. 2c). Unmitigated GHG emissions (SSP3-7.0 and SSP5-8.5) would drive the Great Barrier Reef to a precipitous decline over the century, achieving a near total loss of coral cover by 2080–2100.

Scope for natural adaptation

Despite significant differences among SSPs in the severity and frequency of future heatwaves, coral heat tolerance increases at a similar rate across warming scenarios (Supplementary Fig. 12). The maximum rates of thermal adaptation (1.1–1.4 °C-week per decade) occur in the first half of the century before gradually decelerating, likely constrained by the approaching limit of heat tolerance (8 °C-week). A key indicator of successful adaptation is the persistence of abundant adult populations, particularly among heat-sensitive species that adopt a 'grow fast, die young' strategy (Fig. 3a). Under a global warming scenario 2 °C (SSP1-2.6), heat-sensitive corals can adapt effectively, as evidenced by persistent recovery capabilities driven by their fast growth and high reproductive rates. However, with more severe warming (SSP2-4.5, SSP3-7.0), all coral taxa decline at comparable rates (Fig. 3a, b) because their adaptive capacity is insufficient to keep up with the intensifying selection pressure of rising temperatures. Thus, while it can be expected that reefs will eventually be dominated by the most heat-tolerant taxa[3,5,40], our simulations present a more nuanced picture of future taxonomic composition emergent from the interactive effects of coral demography, connectivity, thermal tolerance and rates of adaptation, which have not yet been teased apart[41,42]. Key to coral persistence is the maintenance of coral brood stocks and reproductive potential that promote fast demographic recovery following bleaching. An encouraging finding is that coral juvenile densities would remain near their historical levels if global warming is kept around 2 °C (Fig. 3c), thus increasing the scope for adaptation and enhancing demographic resilience throughout the century.

Spatial variability of eco-evolutionary responses

Spatial trends in future coral cover exhibit great variability, particularly under relatively modest warming—such as SSP1-2.6 and earlier parts of SSP2-4.5. Mapping the mean state of individual reefs across the weighted ensemble runs (Fig. 4a) reveals large-scale patterns of projected reef health that align with previous studies of thermal refugia and warm spots[43–45]. Thermal refugia were mostly encountered in the southern (Pompey and Swain reef complexes, 20–22 °S) and far-northern (10–12 °S) regions, where localised upwelling brings cool deep water to the surface during austral summer[45]. As a result, thermal refugia allow corals to adapt gradually under mild selective pressure while retaining scope for recovery, thereby enhancing long-term coral persistence. However, while different thermal environments result in different rates of evolution, our projections indicate that the availability of thermal refugia will vanish as warming intensifies (SSP2-4.5,

https://doi.org/10.1038/s41467-025-65015-4

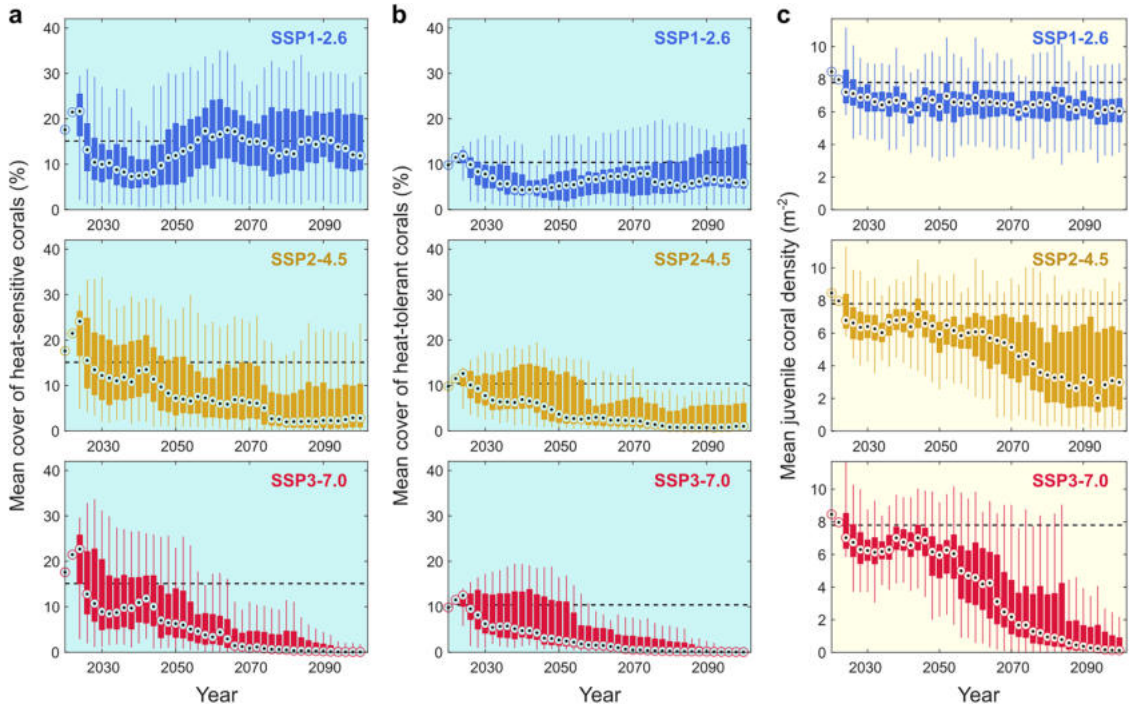

Fig. 3 | Coral demographics under the three most likely warming futures. Ensemble projections of the Great Barrier Reef mean percent cover of heat-sensitive (**a**, four taxonomic groups, including acroporids and pocilloporids) and heat-tolerant corals (**b**, two taxonomic groups, including large massive and submassive/encrusting corals). **c** Projection of mean density of coral juveniles across all groups. See Fig. 2 legend for the description of box-and-whisker plots (n = 20,000 predictions for each biennial distribution). Dashed lines indicate the hindcast (2008–2023) averages for reference.

SSP3-7.0), leading to fewer reefs maintaining high ecological functioning in the second half of the century.

Note that the projected thermal environment was defined at 10-km resolution, but thermal refugia may also exist at finer spatial scales (i.e., within individual reefs). Hence, employing a different coral community model[46] specifically designed to simulate fine-scale (0.5–10 hectares) coral habitats in the Central Great Barrier Reef (Supplementary Methods 2), we find that high levels of heterogeneity also exist at finer spatial resolution among the different sites of a reef (Fig. 4b). Yet, within-reef variability in coral communities may reduce over time as warming affects corals across all sites.

Drivers of eco-evolutionary changes

While a simplification of real-world outcomes (Supplementary Note 1), our model incorporates a complex intertwining of environmental drivers, including cyclones, bleaching events, coral-eating starfish outbreaks, and heterogeneous water quality and larval dispersal. To unravel this complexity, we used statistical linear models of likely ecosystem drivers to evaluate which processes exert the strongest influence on future reef state. We analysed this for two timeframes (Fig. 5a): (1) the mid-century, when stress peaks for low emission scenarios, and (2) at the century's end, when emissions scenarios are most divergent. We find that decreases in the intensity and frequency of coral bleaching—such as those associated with thermal refugia—are most important in promoting total coral cover compared to other disturbances (cyclones, water quality and outbreaks of *Acanthaster* spp.). Indeed, defining thermal refugia and warm spots as representing, respectively, the lower 10th percentile and upper 90th percentile of annual DHW, we find that reefs with higher coral cover are far more common in the cooler refugia (Fig. 5b), especially under mild warming (SSP1-2.6, and SSP2-4.5/SSP3-7.0 by mid-century).

We also find a noticeable influence of coral connectivity, either expressed as larval sink strength derived from raw connectivity data or as simulated number of larvae supplied over the past 5 years (Fig. 5a). This influence is more pronounced under moderate warming (SSP1-2.6), underscoring the compounded effect of heat stress, which diminishes the benefits of larval supply by shortening the periods of recovery. By defining larval barrens and larval hubs as the lower 10th vs. upper 90th percentiles of the annual external larvae supplied, we observe that higher coral cover is more commonly achieved in larval hubs across all warming scenarios (Fig. 5c). This suggests that external larval supply functions as a form of demographic rescue, which is consistent with previous findings using large-scale connectivity[41,42,47]. Moreover, focusing on warm spots reveals that reefs with greater access to external larvae tend to fare better than those with reduced upstream connections, even in the face of high bleaching mortality (Supplementary Fig. 13a). Yet, the ability of larval dispersal to support coral populations diminishes under higher GHG emissions, particularly towards the end of the century. The disruption to reef state becomes so patchy and severe that larval supply is increasingly influenced by local retention and occasional dispersal from upstream reefs that retain enough adult corals.

Corals in warm spots and thermal refugia exhibit adaptation to their respective thermal environments. By mid-century, the mean thermal tolerance of corals on refuge reefs is 1–2 °C-week lower than that of corals in warm spots (Fig. 6a). As warming worsens, either over time or across SSPs, the range of mean heat tolerance broadens in cooler regions, driven by a higher prevalence of cooler-adapted phenotypes. However, this does not imply that heat-tolerant phenotypes are absent in thermal refugia. In fact, refuge reefs, which support vastly greater coral abundance compared to warm spots (Fig. 5b), have a greater reproductive capacity, allowing them to produce larger quantities of coral offspring, including heat-tolerant phenotypes, though in smaller proportions. The larger volume of larvae means that the absolute number of heat-tolerant phenotypes can still be relatively high. Thus, cooler regions are still able to

https://doi.org/10.1038/s41467-025-65015-4

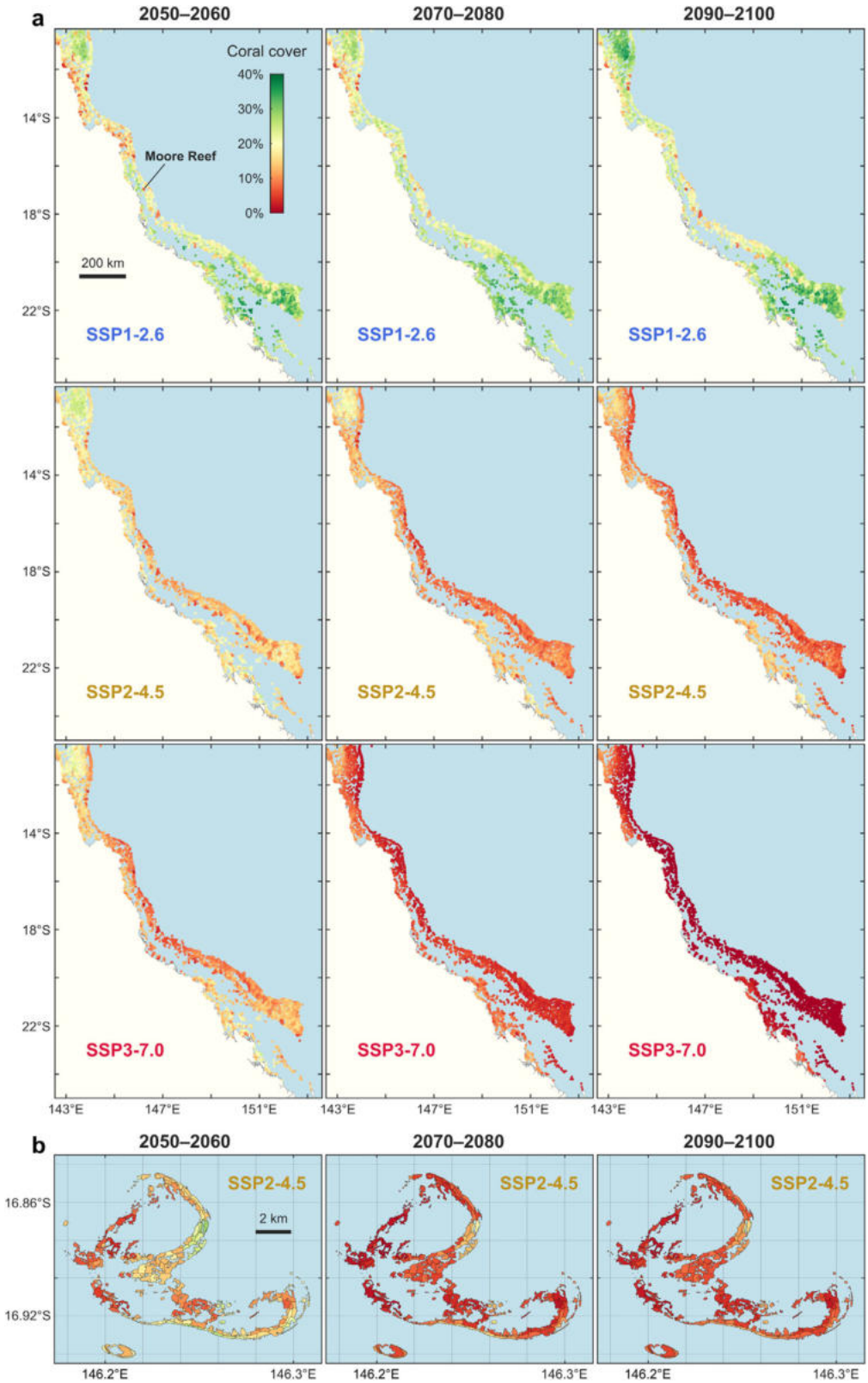

Fig. 4 | Spatial variability and the progressive disappearance of healthy reefs under severe warming. a Annual mean coral cover for 3806 individual reefs across the Great Barrier Reef over three specific decades under SSP1-2.6 (top), SSP2-4.5 (middle) and SSP3-7.0 (bottom). Each reef is represented by a dot located at the centre of its polygon (centroid) (see Fig. 1 legend). **b** Annual mean coral cover for 171 reef habitat sites on Moore Reef in the Central Great Barrier Reef (see location in **a**) predicted by the within-reef, metacommunity model C-scape[48] under SSP2-4.5. Habitat polygons were derived from the Great Barrier Reef Marine Park Authority geospatial data 'GBR10 GBRMP Geomorphic' under licence CC BY 4.0. Annual means were calculated by averaging the predicted coral cover across all bootstrap samples (1000 bootstrap samples of 20 individual model runs).

https://doi.org/10.1038/s41467-025-65015-4

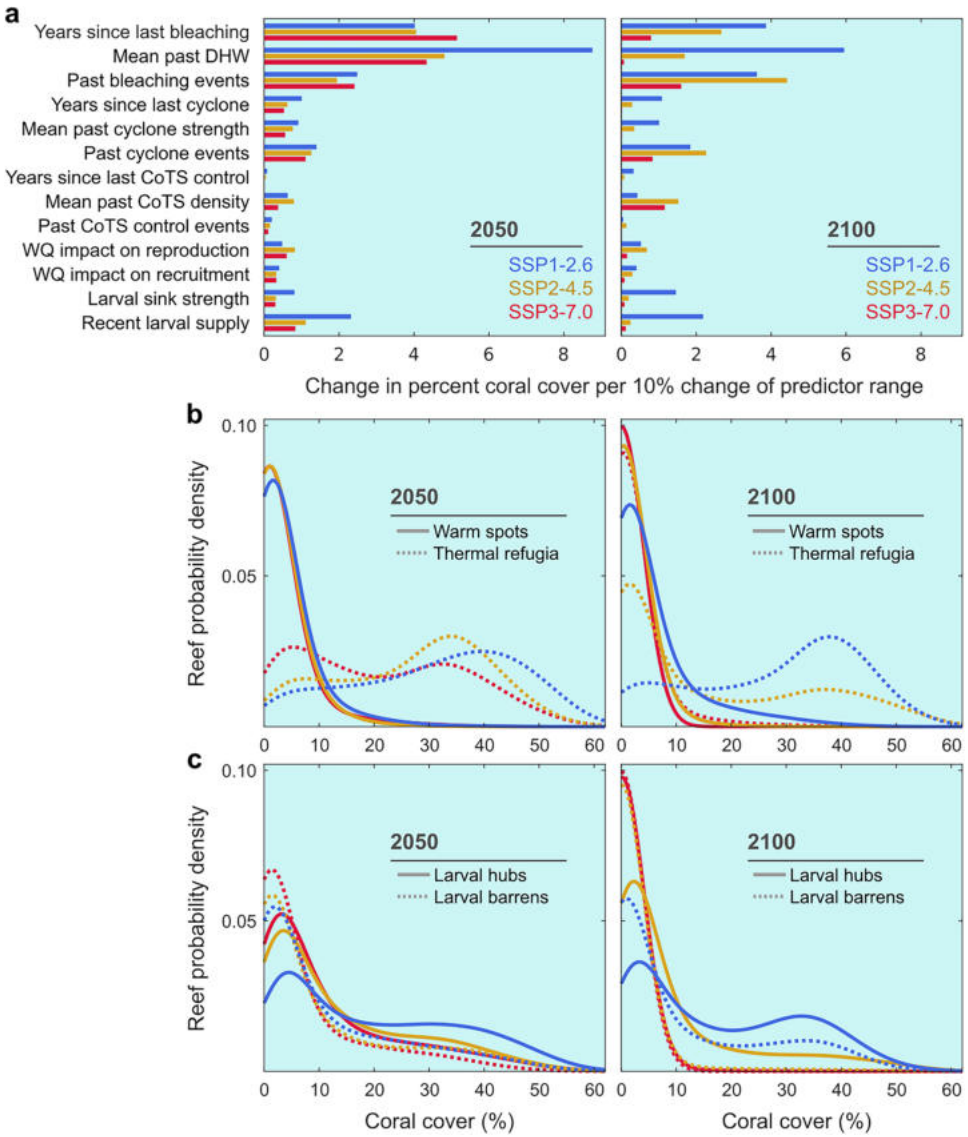

Fig. 5 | Drivers of future coral persistence under plausible global warming. **a** Factors associated with healthier reef outcomes under SSP1-2.6, SSP2-4.5, and SSP3-7.0 for both mid-century (left) and end-century (right) based on predictions of statistical linear models. The influence of each predictor (Supplementary Table 2) is measured by the change in coral cover (as percentage points) for a 10% change of the predictor within its range. The final row represents external larval supply (i.e., excluding local larval retention). CoTS crown-of-thorns starfish (*Acanthaster* spp.), WQ water quality. Probability (kernel) density distribution of reefs based on heat-sensitive coral cover across thermal (**b**, warm spots and thermal refugia) and larval supply (**c**, larval hubs and larval barrens) regimes, excluding reefs impacted by reduced water quality and cyclones in the preceding 5 years (resulting distributions across 200 climate projections: $n = 202{,}570$ reefs in 2050, $n = 205{,}510$ in 2100). Thermal and larval supply regimes are defined, respectively, as those reefs below the 10th or above the 90th percentile for annual DHW and annual amount of external larval supply. Reefs in thermal refugia (i.e., exposed to lowest thermal stress) and in larval hubs (i.e., exposed to highest larval supply) exhibit higher levels of coral cover compared to warm spots and larval barrens. Thermal environments and larval connectivity were calculated as the average heat stress and larval supply experienced in the preceding 5 years. Larval supply excludes local retention and only captures larvae from external source reefs. Colours of SSPs as in (**a**).

disperse warm-adapted phenotypes to some of the reefs where they are needed.

Lastly, we note that larval barrens and hubs display fairly similar distributions of mean heat tolerance, particularly by mid-century (Fig. 6b and Supplementary Fig. S13b). While one might expect that larval connectivity could hinder thermal adaptation by introducing maladapted, cooler phenotypes from thermal refugia[48], our simulations indicate that larval supply has no apparent influence on local adaptation in the mid-term. By the end of the century, larval hubs tend to support slightly higher proportions of heat-tolerant phenotypes, likely due to the influence of upstream reefs that still maintain functional reproductive populations—those that have successfully adapted to warming. However, with the majority of coral populations severely depleted by this time, the potential for genetic rescue through larval connectivity seems to offer limited benefits in the long term.

Discussion

As global warming intensifies, we observe a progressive homogenisation of reef state across multiple spatial scales on the Great Barrier Reef. First, the system-wide average reef state deteriorates, marked by a decline in mean total coral cover in the near term, across all emissions scenarios (Fig. 2b). Second, the spatial variability of reef health gradually reduces as the geographical footprint of recurrent marine heatwaves broadens (Fig. 4a). This can be illustrated by observing a

https://doi.org/10.1038/s41467-025-65015-4

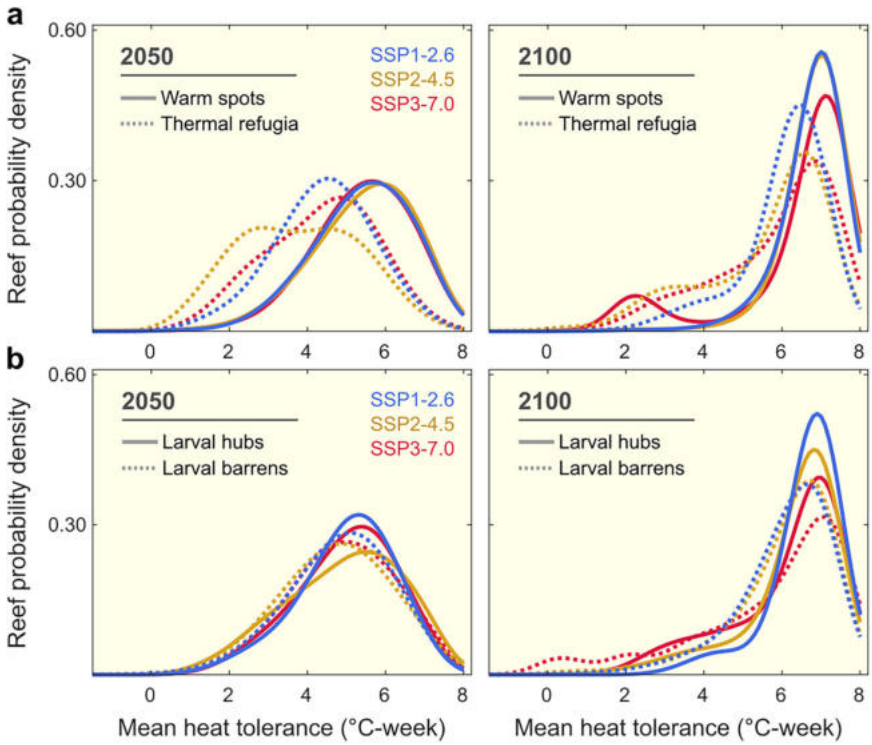

Fig. 6 | Influence of thermal refugia and larval supply and coral adaptation. Probability density distribution of reefs based on mean heat tolerance of heat-sensitive coral taxa across thermal (**a**) and larval supply (**b**) regimes (see definition in Fig. 5 legend) for both mid-century (left) and end-century (right). Heat tolerance is defined as the relative accumulated heat stress (± °C-week) a coral colony can withstand compared to the present-day mean response of its taxonomic group (0 °C-week). Recurrent heatwaves progressively shift the mean tolerance on a reef by selecting corals with the highest heat tolerance (within biological limits set to ± 8 °C-week) over multiple generations. Reefs in thermal refugia slow down the evolution of heat tolerance yet support a greater diversity of heat tolerance values; warm spots achieve greater heat tolerance values at the price of reduced population sizes and lower phenotypic diversity.

single realisation of the future, where the diversity of coral cover trajectories among individual reefs becomes constrained towards the end of century (Supplementary Fig. 1c). Finally, use of a complementary fine-scale ecosystem model parameterised for reef sites within a small reef cluster finds a progressive loss of coral heterogeneity among sites (Fig. 4b). A loss of heterogeneity across multiple spatial scales could be critically important in ways that are not yet fully understood or incorporated into models. For example, patches of relatively healthy habitat with high coral densities are less likely to experience Allee effects in fertilisation[49]. Their progressive loss will undermine the reproductive success of corals within reefs. Yet, it is important to emphasise that coral communities show ability to recover from the initial decline under stringent mitigation targets (<2 °C, SSP1-1.9 and SSP1-2.6). Perhaps more importantly, coral cover entered a trajectory of recovery when temperatures were still rising (i.e., before mid-century). This is an encouraging finding since it suggests that coral adaptation is possible, provided that the rate of temperature change does not exceed the pace of thermal evolution in corals, which is constrained here by life-history, trait heritability and inter-reef connectivity. This result reaffirms the critical importance of climate policy commitments and the urgency of their implementation to curb the rate of warming before 2050.

Our model incorporates key components of natural selection: trait variation, survival of individuals with advantageous traits, and transgenerational inheritance of trait values. Although our parameterisation allows bleaching sensitivity to vary among taxa (Supplementary Fig. 2C, ref. 40), we note that the variation amongst thermal phenotypes, the foundation upon which natural selection operates, was parameterised from one of the more sensitive coral taxa (*Acropora* spp.) as this was the most comprehensive data available[22]. We expanded the limits of heat tolerance within each modelled group to account for the variability conferred by multiple species. However, the lack of data for other taxa introduces additional uncertainty to these limits, which significantly influences eco-evolutionary projections (Supplementary Figs. 14–16). Hence, it is unclear how the scope for thermal adaptation varies across taxa and much remains to be understood about the mechanisms of adaptation itself[50,51]. Specifically, our model does not account for other life history traits that may be affected by rising temperatures[52] or by the strengthening of thermal resistance[53], nor does it capture the evolutionary response of symbiont populations to warming, which influences coral growth and heat tolerance[54].

Beyond these simplifying assumptions, we identified a possible warm bias in our downscaled projections of heat stress. Consequently, the predicted global decline in coral cover during the first 15 years of the forecast may be overestimated, although this must be weighed against other model uncertainties, many of our assumptions favouring optimistic outcomes in the simulated coral demographics (Supplementary Note 1). Overall, there was considerable variation in warming projections across the CMIP6 models, leading to a high level of uncertainty around mean coral cover trajectories, both within and between emission scenarios. Given the many uncertainties associated with the response of corals to climate change, we point out that the uncertainty in our model projections increases substantially over time, largely in ways that are difficult to quantify.

The extent to which coral reefs will maintain their function in the coming decades will not only depend on the ability of corals to adapt to rapid warming, but also on our commitment to mitigate GHG emissions and our capacity to implement effective and efficient management strategies. While reducing GHG emissions remains a top

priority for the protection of coral reefs, opportunities exist for meaningful management interventions that promote coral adaptation and resilience, even under middle-of-the-road GHG emissions (SSP2-4.5). By underpinning key mechanisms that drive coral adaptation across a rapidly changing environment, our model can help prioritising multiple interventions, such as protection against local stressors (fishing, coral-eating starfish outbreaks, reduced water quality) and also reef rehabilitation[12,55]. To this end, identifying reefs that promote demographic and evolutionary rescue at regional scales is crucial. Protecting thermal refugia may help supporting ecosystem functioning locally while maintaining a greater diversity of phenotypes. Conservation efforts, however, must also include areas under strong selective pressure (i.e., warm spots) to foster genetic adaptation[56–58]. The design of conservation strategies that promote adaptation is in its infancy, but one complication is the potential for 'gene swamping' where the dispersal of cool-adapted corals into warm spots could slow adaptation[48,56,59]. However, while the potential exists for such disruption on the Great Barrier Reef—where 13% of reefs that constitute refugia from bleaching can disperse corals to 58% of the whole ecosystem[43]—we did not find evidence of a lack of adaptation in thermal refugia and a negligible influence of larval supply on local adaptation. Thus, our model projections indicate that management strategies for adaptation that encompass multiple thermal environments can be flexible and unconstrained by patterns of larval supply. In fact, larval hubs should be prioritised for building reef resilience since areas with high larval supply are likely to be more resilient even under moderate GHG emissions. Conversely, areas lacking larval supply might be considered for rehabilitation measures. Ultimately, continued investment in reef management is essential even if we move towards lower GHG emissions.

Methods

Coral-reef ecosystem modelling

Coral projections under future warming were performed using ReefMod-GBR[20], a coral individual-based model that simulates coral metacommunity dynamics throughout the ~2300 km length of Australia's Great Barrier Reef (GBR). The model tracks the size of individual coral colonies of six taxonomic/morphological groups under the influence of demographic processes, ecological interactions and disturbances: acroporids (arborescent, plating and corymbose), pocilloporids, large massive corals and submassive/encrusting corals. Coral demography is simulated with a seasonal time step of 6 months (austral summer: from November to April; austral winter: from May to October) using rates of recruitment, growth, survival and fecundity characteristic of ~5–10 m deep reef environments. Metacommunity dynamics are captured by tracking the dispersion and settlement of coral larvae throughout a network of 3806 individual reefs (Supplementary Fig. 1a). Most processes are stochastic at the colony or reef level, reflecting local variability in demographics and disturbance exposure.

The model simulates the major acute stressors responsible for widespread coral mortality across the GBR[20]: temperature-induced mass coral bleaching (detailed below), tropical cyclones, and outbreaks of the coral-eating crown-of-thorns starfish (*Acanthaster* spp., CoTS). Cyclone-induced coral mortality is taxa- and colony-size specific, with mortality rates predicted based on cyclone intensity (Saffir-Simpson scale). CoTS-induced mortality is taxa-specific, with fast-growing corals more susceptible. CoTS outbreaks are simulated using an age-structured metapopulation model, and coral mortality is determined by CoTS abundance at a reef, calculated using CoTS age-specific consumption rates. Additional stressors include reduced water quality (suspended sediment), which hinders coral recruitment, and loose coral debris generated by acute disturbances, which hinders the survival of recruits, jointly impeding coral recovery.

The model has provided credible reconstructions of recent coral cover trends observed across the GBR[20]. Subsequent applications have explored possible coral futures under climate projections of the fifth phase of the Coupled Model Intercomparison Project (CMIP5) and for different scenarios of reef management[60–62]. We further developed the model with (1) the evolutionary dynamics of coral heat tolerance under selection by heat stress (i.e., mass coral bleaching) and (2) the most up-to-date climate projections (CMIP6) derived from a wider array of greenhouse gas (GHG) emissions. This spatially-explicit, eco-evolutionary model enables us to simulate the potential for coral adaptation under a range of future scenarios of warming across GBR coral communities. The code of the model (ReefMod-GBR v.7.0) is archived in the Zenodo public repository (https://doi.org/10.5281/zenodo.16734996).

Model domain and reef definition

An individual reef is represented by a grid lattice of 20 × 20 cells, each cell approximating 1 m^2 of the reef substratum. The associated disturbance regime is reconstructed from past exposure (2008–2023) to cyclones, bleaching and suspended sediment concentrations (Supplementary Fig. 1b) inferred at resolutions finer than 10 km (see ref. 20 for a detailed description). Here, the area suitable to coral colonisation was refined for each reef individually using high-resolution (10 m) reef mapping derived from remote sensing (Supplementary Methods 1). First, an estimate of the 3D surface area of hard reef substrate (down to 20 m depth) was calculated based on reef geomorphological and bathymetry maps[63]; this produced a total area of coral habitat of 13,842 km^2 for the entire GBR. During simulations, the density of coral and CoTS larvae produced after spawning on the grid lattice of a reef is multiplied by the 3D surface area of that reef to scale up to the amount of larvae produced before dispersal. Second, the proportional area of coral habitat that can be colonised was evaluated based on maps of benthic cover types[63]; this sets a limit to coral colonisation on each individual reef. Coral and CoTS population connectivity among all individual reefs was derived from biophysical simulations of coral and CoTS larval dispersal following annual spawning events across the reef network[20,64].

Bleaching-induced mortality

Coral mortality caused by bleaching is modelled as a function of accumulated heat stress expressed as Degree Heating Week (DHW, unit: °C-week). Bleaching occurs during the austral summer when DHW ≥ 3 °C-week on any given reef[5], but is prevented if a cyclone also occurs in the season[65]. First, a probability of initial mortality m is estimated from a regression model[20] fitted to GBR observations collected at the peak of the 2016 mass-bleaching event[5], further extended to account for the sensitivity of multiple taxa at different depths:

$$m = w \cdot s \cdot [\exp(0.168 + 0.347 \cdot \mathrm{DHW}) - 1]/100 \quad (1)$$

where w is a depth-related attenuation coefficient of heat stress and s is a sensitivity coefficient for specific taxa. With $w = 1$ and $s = 1$, Eq. (1) predicts the community-level response recorded at 2 m depth. Coefficient w is modelled (Supplementary Fig. 2a) using observations of bleaching mortality collected in the Northern GBR along a depth profile of light attenuation[66]:

$$w = (0.420 + 0.272 \cdot d)^{-1} \quad (2)$$

We modelled reefs at an average depth of 7 m, considering the modelled coral demographics are representative of 5–10 m forereef environments, thus effectively fixing w to 0.43. The sensitivity coefficient s was determined based on observed taxon-specific responses to bleaching[5] and ranges between 0.25–1.70 (ref. 20).

In a second step, initial mortality m is capped to 1 and extended to include subsequent mortality occurring after the peak of the bleaching event. A previous calibration[20] found that the long-term (8 months) losses of percent coral cover reported on the GBR following the 2016 mass bleaching[5] can be reproduced by simulation with the following transformation:

$$M = 1 - (1 - m)^6 \quad (3)$$

where M is the probability of total mortality within each taxonomic group. This transformation confers a sigmoid shape to the DHW/mortality relationship (Supplementary Fig. 2b), which sets 50% coral mortality at ~8 °C-week and ~13 °C-week for heat-sensitive (the three acroporid groups and pocilloporids) and heat-tolerant taxa (large massive and submassive/encrusting corals), respectively (Supplementary Fig. 2c).

Heat tolerance of individual corals

Significant variation in heat tolerance can occur among corals of the same species within a specific thermal environment[22,67,68]. To capture this variability within a taxonomic group, we define the heat tolerance (HT) of a coral colony as a quantitative trait that reflects its relative ability to survive heat stress[22] compared to the group mean survival rate, i.e., the representative DHW/mortality relationship of the group at initialisation. Specifically, HT measures the difference in the amount of accumulated heat stress (±°C-week) that a coral colony can withstand compared to the group mean response:

$$m = w \cdot s \cdot (\exp[0.168 + 0.347 \cdot (\mathrm{DHW} - \mathrm{HT})] - 1)/100 \quad (4)$$

This essentially shifts the curve of initial mortality along the axis of DHW values: a positive and negative HT value confers lower and higher bleaching mortality, respectively, compared to the group mean for the same DHW value. It can be re-written as:

$$m = w \cdot s \cdot \exp(0.168 + 0.347 \cdot \mathrm{DHW} - 0.347\mathrm{HT})/100 - w \cdot s/100 \quad (5)$$

The term $w \cdot s/100$ being negligible (<0.01, less than 1% mortality), a fair approximation is:

$$m = w \cdot s \cdot \exp(-0.347 \cdot \mathrm{HT}) \cdot \exp(0.168 + 0.347 \cdot \mathrm{DHW})/100 \quad (6)$$

Hence, the specific bleaching response of a coral colony can be obtained from Eq. (1) using a new sensitivity coefficient s^* expressed as:

$$s^* = s \cdot \exp(-0.347 \cdot \mathrm{HT}) \quad (7)$$

We assume that HT values at initialisation within a taxonomic group follow a normal distribution of mean 0, which corresponds to the average bleaching sensitivity (s) of that group. To get a realistic estimate of the variability of HT, we used the results of a heat stress experiment performed on the corymbose *Acropora digitifera* collected on a shallow outer reef crest in Palau, Western Pacific Ocean[22]. Coral fragments were exposed to an increasing temperature and assessed for signs of heat stress, allowing the modelling of a 0–1 index of bleaching and mortality (BMI) as a function of daily DHW values. As a result, there was a difference of 4.8 °C-week (3.1–6.8 °C-week 95% confidence interval) between the 10th and 90th percentiles of the population measured at the cut-off BMI level of 0.12 (i.e., 12% mortality). Assuming the BMI is a functional equivalent to M, we infer that this difference is ~6.4 °C-week at 100% mortality (Supplementary Fig. 3a). For a standard normal distribution, the 90th percentile has a score of ~1.28. Therefore, a normal distribution of mean zero and a 90th percentile score of 6.4/2 has a standard deviation of 6.4 / (2 × 1.28) = 2.5. We thus assume that present-day HT values follow a normal distribution of mean zero and standard deviation $\sigma = 2.5$ °C-week within each taxonomic group. At initialisation, a value is drawn from this distribution (Supplementary Fig. 3b) for each created coral. Corals retain their assigned HT throughout their lifetime. When bleaching occurs, a probability of mortality is calculated for every colony following Eqs. (1)–(3) and (7), and survivors are determined by binomial draws.

Because a normal distribution has tails extending to infinity, negative and positive limits to HT ($\pm \mathrm{HT}_{\max}$) are required to avoid creating unrealistic heat tolerance values. A range based on the 1st and 99th percentiles of the distribution observed in ref. 22 would set bounding limits to approximately −6 and +6 °C-week (Supplementary Fig. 3b). Yet, this distribution is derived from experimental data gathered for a single species with a limited number of individuals. When extrapolating to multiple taxa, it is reasonable to assume a wider range of heat tolerance values. We extended this range by 2 °C-week on either side of the distribution (i.e., $|\mathrm{HT}_{\max}| = 8$ °C-week) to capture some additional level of variability among species within a modelled group. Due to the lack of empirical data on heat tolerance for other coral taxa—comparable to the values reported in ref. 22—there is significant uncertainty in extrapolating heat tolerance variability across multiple species. Furthermore, extreme thermal phenotypes could emerge in the future from the complex interactions among mechanisms of selection, acclimation and genetic mutations. As additional data become available for a broader range of taxa, and further progress on our understanding of adaptive mechanisms, it will become possible to more accurately represent the potential range of heat tolerance values.

Cross-generational heritability of heat tolerance

Thermal adaptation occurs as a trans-generational response to natural selection driven by mass bleaching and mortality events. Inheritance of heat tolerance is modelled based on the narrow-sense heritability (h^2), which measures the proportion of variation in this trait that is attributable to additive genetic effects (i.e., those genetic effects that are inherited, as opposed to dominance and epistasis)[69,70]. As such, heritability expresses the similarity of thermal phenotypes between parents and offspring, and being a proportion, is confined from 0 (offspring and parental phenotypes are unrelated) to 1 (perfect transmission of parental phenotypes). Based on empirical estimates[24,25], we set $h^2 = 0.3$ for the heritability of heat tolerance and assume it constant in space and time (but see ref. 69). To determine thermal phenotypes (i.e., HT) in coral offspring, we first predict the mean heat tolerance of the new generation from the selected parents following the univariate breeder's equation[71,72]:

$$R = h^2 \cdot S \quad (8)$$

where R is the per generation response to selection expressed as the change in mean heat tolerance in the next generation and S is the selection differential (i.e., the change in mean heat tolerance after selection within the parental population). Specifically, S (°C-week) within each taxonomic group is estimated at every time step t as:

$$S_t = \mathrm{HT}_{P,t} - \mathrm{HT}_{P,t-1} \quad (9)$$

where HT_P is the mean heat tolerance of adult colonies weighted by the amount of their respective reproductive outputs (function of colony size, as per ref. 20), such that colonies with greater fecundity contribute more to the mean parental phenotype. Assuming the offspring phenotypes (HT_O) are normally distributed, their mean value is obtained by adding the generational response to selection to the mean parental phenotype before selection:

$$\mathrm{HT}_{O,t} \sim \mathrm{N}(\mathrm{HT}_{P,t-1} + R_t, \mathrm{var}(\mathrm{HT}_{P,t})^{1/2}) \quad (10)$$

Note the variance of heat tolerance in the population of offspring is assumed to match the fecundity-weighted variance of parental phenotypes after selection, based on the expectation that phenotypic variance is reduced under strong selective pressure. In the particular case where no gravid colonies were present at t − 1, $HT_{P,\,t-1}$ was set to 0, meaning that the selection differential was calculated relative to the present-day distribution of heat tolerance.

Since corals produce millions of offspring, the computation is only performed for a representative sample of 1000 offspring HT phenotypes per taxonomic group per reef. The sampled HT phenotypes are then dispatched across the reef network according to probabilities of larval dispersal specified in connectivity matrices. Practically, a pool of 1000 incoming HT phenotypes is created for any given sink reef by sampling within each pool of outgoing HT phenotypes (i.e., at the reefs of origin) proportionally to the associated source-sink dispersal probability. Hence, the distribution of HT phenotypes within a pool of incoming larvae reflects the contribution of each source reef to larval supply[73] A coral recruit is then assigned one of the incoming HT phenotypes through random sampling (with replacement).

Historical regime of environmental forcing

The model first simulates the recent (2008–2023) dynamics of coral and CoTS populations from temporally- and spatially-realistic environmental regimes[20] (Supplementary Fig. 1b). To ensure model simulations accurately reflect real-world conditions, the cover of each coral taxonomic group at each individual reef is initialised based on historical observations from monitoring data (see details in ref. 20). As in previous applications of the model, coral and CoTS larval connectivity (i.e., source-sink dispersal probability) is derived from biophysical simulations of larval dispersal[64,74] performed over six spawning seasons (water year 2010, 2011, 2012, 2014, 2015 and 2016) using a three-dimensional hydrodynamic model of the GBR[75]. For corals, larval particles were released at actual spawning dates following historical observations of mass coral spawning across the GBR, resulting in a total of 25 simulated spawning events[74]. For CoTS, four spawning events were simulated for each spawning season[64]. For both coral and CoTS, connectivity matrices from multiple spawning events were combined to create a single matrix for each of the six water years (see details in refs. 64,74). The resulting annual connectivity matrices were applied as a recursive chronological sequence over the 2008–2023 period[20]. Past exposure to cyclones was reconstructed from sea-state predictions of wave height[26] paired with estimates of cyclone category inferred from the closest distance to actual cyclone tracks[76]. Historical heat stress was determined from satellite-derived records of maximum annual DHW at 5-km resolution from NOAA Coral Reef Watch[21]. Suspended sediment concentrations were inferred from 2010–2018 simulations of the eReefs coupled hydrodynamic-biogeochemical model[75,77]. CoTS management was simulated by culling CoTS populations on a per reef basis[60] following the CoTS Control Program implemented across the GBR Marine Park. Hindcast coral cover reconstructions between 2008–2023 were simulated by repeating 20 stochastic runs of the historical environmental regime. In each run, normally-distributed noise was injected into the mechanisms of population initialisation, recruitment and mortality events across individual reefs. This process generates demographic fluctuations reflecting the natural variability of reef populations.

Forecast scenarios of environmental forcing

Scenarios of future heat stress during the twenty-first century were developed using an ensemble of coupled atmosphere-ocean general circulation models (AOGCMs) of the CMIP6 database[29]. AOGCMs simulate possible future climates at regional scales under the Shared Socioeconomic Pathway (SSP) framework, a set of alternative scenarios of societal and economic development leading to different trajectories of atmospheric carbon concentrations[10]. We extracted climate projections simulated daily between 2014 and 2100 by ten AOGCMs (Supplementary Table 1) under five scenarios of GHG emission entailed in the last Intergovernmental Panel on Climate Change (IPCC) Assessment Report[1] (SSP1-1.9, SSP1-2.6, SSP2-4.5, SSP3-7.0, SSP5-8.5). SSP1-1.9 and SSP1-2.6 are two scenarios of strong mitigation, in which global warming by 2100 is limited to 1.5 °C and 2.0 °C above preindustrial (1850–1900) levels in line with the 2015 Paris Agreement targets. SSP2-4.5 is an intermediate scenario in which GHG emissions remain around contemporary levels until the middle of the century, with end-of-century warming estimates around 2.7 °C above pre-industrial temperatures. SSP3-7.0 and SSP5-8.5 are non-mitigation scenarios with atmospheric carbon concentrations doubling from current levels by 2100 and 2050, respectively, leading to global warming around 3.6 °C and 4.4 °C.

As a result, an ensemble of 47 climate realisations were available at coarse spatial resolution (80–500 km), with SSP1-1.9 being only available for seven AOGCMs (Supplementary Table 1). Each daily warming projection was downscaled to 10 km using semi-dynamical shelf-sea modelling across the 0–50 m depth range[30,78]. Briefly, surface-level atmospheric variables predicted by AOGCMs were combined with high-resolution bathymetry and tidal forcing to simulate daily sea surface temperatures (SST) based on local physical properties of the water column. For each downscaled SST projection, DHWs were calculated as the daily summation of SST anomalies exceeding 1 °C above the maximum monthly mean temperature (MMM) over a 12-week running window, following ref. 21. The MMM of each 10-km pixel was calculated over the period 1985–2012 from the NOAA Coral Reef Watch climatology[21]. Annual maximum DHWs were calculated over an "austral year" (August to July) to avoid the double counting of bleaching events across two calendar years during austral summers, and assigned to each of the 3806 reefs based on the closest 10-km pixel.

Because only one warming realisation was available for each AOGCM/SSP, the resulting future for any given reef is one series of heat stress events occurring at specific times (i.e., years). To allow for fluctuations in the timing of future coral bleaching, we generated 20 stochastic sequences of heat stress between 2024–2100 for each warming scenario. This was achieved by randomly sampling, without replacement (i.e., shuffling), the DHWs predicted for all reefs within each decade, generating an ensemble of 940 stochastic warming futures. By shuffling the DHW years for all reefs together within each decade individually, we ensured that the spatial distribution of heat stress was preserved for any given DHW year, while maintaining the long-term warming trend forecasted by each climate model.

Each of the 20 stochastic DHW futures of a given AOGCM/SSP was paired with one of the 20 stochastic hindcast reconstructions and one specific timeseries of 20 stochastic future (2024–2100) of cyclone tracks[79]. Applying the same scenarios of future cyclones with each AOGCM/SSP ensures consistency in the comparison of warming scenarios. Hindcast spatial distributions of suspended sediments and coral/CoTS larval connectivity were applied in recursive sequences until the end of the century (Supplementary Fig. 1b).

Ecosystem projection analysis

A key uncertainty in projections of future climate change is the sensitivity of global warming to GHG emissions[80]. Equilibrium Climate Sensitivity (ECS), which quantifies the increase in global temperature resulting from a sustained doubling of CO_2 concentrations, is a standardised measure for comparing the sensitivity of different AOGCMs to changes in GHG forcing[81]. While our selection of AOGCMs covers a broad spectrum of ECS values (2.6 – 5.3 °C, Supplementary Table 1), caution has been raised over the selection of models associated to unrealistically high ECS[38,39]. Equilibrium climate sensitivity is very likely (90% probability) to lie between 2.3–4.7 °C (ref. 82), yet a significant number of CMIP6 models have an ECS value above this range[38,81]. While

the warming projections of these 'hot' models[39] are biased towards the high end, they cannot be ruled out as implausible[81,82].

To avoid biased projections favouring excessive warming, we assessed future reef health and associated uncertainty by assigning weights to each eco-evolutionary simulation based on the likelihood of the ECS of the underlying AOGCM. First, we inferred the relative likelihood of each AOGCM (Supplementary Fig. 11) given its ECS value based on a Bayesian-derived probability distribution of Earth's climate sensitivity[82]. Then, we employed bootstrap sampling within each SSP ensemble of simulations (140 runs for SSP1-1.9, 200 runs for all other SSPs) to randomly select eco-evolutionary runs. In this process, a bootstrap sample for a given SSP comprises 20 runs of the model, one for each scenario of future cyclones paired with one sequence of DHW drawn from the available AOGCMs using the associated likelihood as the weighting factor. This approach ensures that (1) cyclone variability is equally represented across all bootstrap samples, (2) final projections are constrained by the most realistic warming limits and (3) all AOGCMs are considered for a reliable assessment of uncertainty around future warming. A total of 1000 bootstrap samples were constructed for each SSP scenario.

For each individual run, percentage total coral cover, density of coral juveniles (defined as coral diameter between 1–5 cm) and thermal tolerance for each coral taxonomic group was averaged across all individual reefs using their log-transformed area as weight. For every SSP ensemble, these ecological metrics can be tracked through a distribution of 20,000 estimates (20 runs × 1000 bootstrap samples) obtained at yearly intervals from 2008 to 2100.

Drivers of ecosystem changes

In any given simulation, some reefs fare better than others. Our goal here was to identify the drivers of success and compare them among SSPs and between the mid- and late centuries. For each AOGCM and SSP, we took 20 independent simulations of the dynamics of all 3806 reefs until 2100. This resulted in between 532,840 and 761,200 individual reef trajectories per SSP, depending on the number of AOGCMs available. Two census dates were created: 2050 (for mid-century), when stress levels approach maximum for the low emissions scenarios, and 2100 (for late century), when stress levels diverge greatly among SSPs. We then took all simulations for a given time period (e.g., mid-century) and normalised the predictors and response (total coral cover per reef) by *z*-score. Responses were normalised to ignore differences in the absolute cover between census years. Predictors were normalised because of diversity in their units of measurement (Supplementary Table 2). The only exception was the cumulative number of larvae arriving at reefs in the last 5 years due to high variability in z-scores and the need to use the log of larval supply to stabilise variance.

The role of predictors on future reef state was evaluated using simple linear models[83]. We did not include random effects since we did not intend to create a model for future prediction and their incorporation could mask desirable insights. For example, a random (or fixed) effect might help explain why reefs under one climate model fared better, on average, than those under another climate model, but this is a distraction from our perspective; our primary interest is that healthier reefs were associated with, e.g., less frequent bleaching events, which happened to occur less often in some models than others. We do not provide estimates of predictor significance because the data result from models and any variable can become significant with enough simulations.

Predictors of relatively healthy reefs were identified using two methods. First, the explanatory power of the transformed predictor in the linear model, represented by the partial coefficient of determination[84] (R^2). The second was more complex because we wished to provide a comparable measure of the impact of each variable on reef state, recognising that most predictors are measured on different scales. To do this we first rescaled the model coefficient of each predictor so that it reflected units of the original predictor's impact on coral cover. In order to provide some parity among predictors with different units, we rescaled the effect size so that it measured the change in coral cover associated with a 10% increase of the predictor across its range. For example, a result of 4% cover associated with metric X implies that a 10% increase within the range of metric X would increase average coral cover by 4 units of cover, with all else being equal.

Sensitivity analyses

We assessed the sensitivity of future coral cover predictions to the input parameters that most strongly influence the key processes driving eco-evolutionary dynamics and resilience of corals: susceptibility to heat stress, thermal adaptation, recovery potential, larval supply and susceptibility to cyclones and CoTS outbreaks. As a result, 13 parameters were selected (Supplementary Table 3) and two sensitivity analyses were performed.

First, we varied each parameter independently by ± 20% while holding the others constant, simulating a single scenario of future cyclones under three warming projections (SSP1-2.6, SSP2-4.5, SSP3-7.0) of the MIROC-6 climate model. The impact of the change in each parameter was assessed in terms of both absolute (Supplementary Fig. 14) and relative (Supplementary Fig. 15) differences in projected GBR mean coral cover. Among recovery-related parameters, colony growth and maximum settler density had the strongest effects, causing up to ± 35% variation in mean coral cover—equivalent to ± 5 percentage points under SSP1-2.6, and less than 2 percentage points under higher warming, when mean coral cover drops below 10%. Variations in the limits of heat tolerance caused up to ± 30% change in the mean coral cover after mid-century, with broader limits (± 9.6 °C-weeks) improving coral cover up to ~5 percentage points under SSP1-2.6. In contrast, changes in the heritability of heat tolerance had minimal impacts. Variations in depth-attenuation of DHW and the spread (standard deviation) of naive heat tolerance led to ± 20% variation (± 2.5 percentage points under SSP1-2.6). Parameters controlling the impact magnitude of cyclones and CoTS had marginal effects.

Second, a global sensitivity analysis was conducted to assess the influence of each parameter in the context of interactions with others. Here, 100 simulations of the same SSP1-2.6 scenario were run, randomly sampling all parameters from uniform distributions within their ± 20% range. Parameter influence was captured by fitting a linear model to the resulting relative changes in GBR mean coral cover ($n = 100$ predictions) extracted at different time points (Supplementary Fig. 16). Colony growth and maximum settler density remained the most influential parameters throughout the century, with mean effects up to ±25% and ±16%, respectively. The influence of heat tolerance limits increased over time, reaching ±17% by the end of the century. Depth attenuation of DHW and the spread of naive heat tolerance had mean effects up to ±9%. Notably, cyclone impact magnitude had a substantial effect (±18%)—undetected in the first analysis—suggesting significant interactions with other parameters.

Reporting summary

Further information on research design is available in the Nature Portfolio Reporting Summary linked to this article.

Data availability

Data used and produced by this study are available at the GitHub repository https://github.com/ymbozec/GBR.7.0_Futures_CMIP6[85]. Maps were created using the geospatial datasets 'Great Barrier Reef Features (GDA94)' (Figs. 1a and 4a) and 'GBR10 GBRMP Geomorphic' (Fig. 4b) provided by the Great Barrier Reef Marine Park Authority's Reef Geohub platform (https://reef-geohub-ext-geohubgbrmpa.hub.arcgis.com/).

Code availability

The code of ReefMod-GBR developed for this analysis is available at the GitHub repository https://github.com/ymbozec/REEFMOD.7.0_GBR[86]. All figures and analyses supporting the findings of this paper can be reproduced with the code and data available at the GitHub repository https://github.com/ymbozec/GBR.7.0_Futures_CMIP6[85].

References

1. Intergovernmental Panel on Climate Change (IPCC). Summary for policymakers. in *Climate Change 2021: The Physical Science Basis. Contribution of Working Group I to the Sixth Assessment Report of the Intergovernmental Panel on Climate Change* (eds Masson-Delmotte, V. et al.) 3–32 (Cambridge University Press, 2021).
2. Hughes, T. P. et al. Spatial and temporal patterns of mass bleaching of corals in the Anthropocene. *Science* **359**, 80–83 (2018).
3. Hoegh-Guldberg, O. et al. Coral reefs under rapid climate change and ocean acidification. *Science* **318**, 1737–1742 (2007).
4. Eakin, C. M. et al. Caribbean corals in crisis: record thermal stress, bleaching, and mortality in 2005. *PLoS ONE* **5**, e13969 (2010).
5. Hughes, T. P. et al. Global warming transforms coral reef assemblages. *Nature* **556**, 492 (2018).
6. Brown, B. E. Coral bleaching: causes and consequences. *Coral Reefs* **16**, S129–S138 (1997).
7. Baker, A. C., Glynn, P. W. & Riegl, B. Climate change and coral reef bleaching: an ecological assessment of long-term impacts, recovery trends and future outlook. *Estuar. Coast. Shelf Sci.* **80**, 435–471 (2008).
8. Skirving, W. J. et al. The relentless march of mass coral bleaching: a global perspective of changing heat stress. *Coral Reefs* **38**, 547–557 (2019).
9. Sully, S., Burkepile, D. E., Donovan, M. K., Hodgson, G. & Van Woesik, R. A global analysis of coral bleaching over the past two decades. *Nat. Commun.* **10**, 1264 (2019).
10. Lee, J.-Y. et al. Future global climate: scenario-based projections and near-term information. in *Climate Change 2021: The Physical Science Basis. Contribution of Working Group I to the Sixth Assessment Report of the Intergovernmental Panel on Climate Change* 553–672 (Cambridge University Press, 2021).
11. Mcleod, E. et al. The future of resilience-based management in coral reef ecosystems. *J. Environ. Manag.* **233**, 291–301 (2019).
12. Bay, L. K., Gilmour, J., Muir, B. & Hardisty, P. E. Management approaches to conserve Australia's marine ecosystem under climate change. *Science* **381**, 631–636 (2023).
13. Klein, S. G. et al. Projecting coral responses to intensifying marine heatwaves under ocean acidification. *Glob. Change Biol.* **28**, 1753–1765 (2022).
14. Mellin, C. et al. Cumulative risk of future bleaching for the world's coral reefs. *Sci. Adv.* **10**, eadn9660 (2024).
15. Van Hooidonk, R. et al. Local-scale projections of coral reef futures and implications of the Paris Agreement. *Sci. Rep.* **6**, 1–8 (2016).
16. McClanahan, T. R. et al. Diversification of refugia types needed to secure the future of coral reefs subject to climate change. *Conserv. Biol.* **38**, e14108 (2024).
17. Bell, G. Evolutionary rescue. *Annu. Rev. Ecol. Evol. Syst.* **48**, 605–627 (2017).
18. Hufbauer, R. A. et al. Three types of rescue can avert extinction in a changing environment. *Proc. Natl. Acad. Sci. USA* **112**, 10557–10562 (2015).
19. Hughes, T. P. et al. Global warming impairs stock–recruitment dynamics of corals. *Nature* **568**, 387–390 (2019).
20. Bozec, Y.-M. et al. Cumulative impacts across Australia's Great Barrier Reef: a mechanistic evaluation. *Ecol. Monogr.* **92**, e01494 (2022).
21. Skirving, W. et al. CoralTemp and the coral reef watch coral bleaching heat stress product suite version 3.1. *Remote Sens.* **12**, 3856 (2020).
22. Humanes, A. et al. Within-population variability in coral heat tolerance indicates climate adaptation potential. *Proc. R. Soc. B* **289**, 20220872 (2022).
23. Richards, T. J. et al. Moving beyond heritability in the search for coral adaptive potential. *Glob. Change Biol.* **29**, 3869–3882 (2023).
24. Bairos-Novak, K. R., Hoogenboom, M. O., van Oppen, M. J. & Connolly, S. R. Coral adaptation to climate change: meta-analysis reveals high heritability across multiple traits. *Glob. Change Biol.* **27**, 5694–5710 (2021).
25. Humanes, A. et al. Selective breeding enhances coral heat tolerance to marine heatwaves. *Nat. Commun.* **15**, 8703 (2024).
26. Puotinen, M., Maynard, J. A., Beeden, R., Radford, B. & Williams, G. J. A robust operational model for predicting where tropical cyclone waves damage coral reefs. *Sci. Rep.* **6**, 26009 (2016).
27. Castro-Sanguino, C. et al. Coral composition and bottom-wave metrics improve understanding of the patchiness of cyclone damage on reefs. *Sci. Total Environ.* **804**, 150178 (2022).
28. Australian Institute of Marine Science. AIMS-LTMP and MMP Coral Reef Monitoring Modelled Output. https://doi.org/10.25845/q40d-7a72 (2021).
29. Eyring, V. et al. Overview of the Coupled Model Intercomparison Project Phase 6 (CMIP6) experimental design and organization. *Geosci. Model Dev.* **9**, 1937–1958 (2016).
30. McWhorter, J. K. et al. The importance of 1.5 °C warming for the Great Barrier Reef. *Glob. Change Biol.* **28**, 1332–1341 (2022).
31. Rogelj, J. et al. Paris Agreement climate proposals need a boost to keep warming well below 2 °C. *Nature* **534**, 631–639 (2016).
32. Meinshausen, M. et al. Realization of Paris Agreement pledges may limit warming just below 2 °C. *Nature* **604**, 304–309 (2022).
33. Raftery, A. E., Zimmer, A., Frierson, D. M., Startz, R. & Liu, P. Less than 2 °C warming by 2100 unlikely. *Nat. Clim. Change* **7**, 637–641 (2017).
34. Vargas Zeppetello, L. R., Raftery, A. E. & Battisti, D. S. Probabilistic projections of increased heat stress driven by climate change. *Commun. Earth Environ.* **3**, 183 (2022).
35. Liu, G., Strong, A. E. & Skirving, W. Remote sensing of sea surface temperatures during 2002 barrier reef coral bleaching. *Eos Trans. Am. Geophys. Union* **84**, 137–141 (2003).
36. NOAA Coral Reef Watch. Methodology, product description, and data availability of NOAA Coral Reef Watch's version 3.1 daily global 5km satellite coral bleaching heat stress monitoring products. https://coralreefwatch.noaa.gov/product/5km/methodology.php. (Accessed 13 Oct 2025).
37. Hughes, T. P. et al. Emergent properties in the responses of tropical corals to recurrent climate extremes. *Curr. Biol.* **31**, 5393–5399 (2021).
38. Tokarska, K. B., Hegerl, G. C., Schurer, A. P., Forster, P. M. & Marvel, K. Observational constraints on the effective climate sensitivity from the historical period. *Environ. Res. Lett.* **15**, 034043 (2020).
39. Hausfather, Z., Marvel, K., Schmidt, G. A., Nielsen-Gammon, J. W. & Zelinka, M. Climate simulations: recognize the 'hot model' problem. *Nature* **605**, 26–29 (2022).
40. van Woesik, R., Sakai, K., Ganase, A. & Loya, Y. Revisiting the winners and the losers a decade after coral bleaching. *Mar. Ecol. Prog. Ser.* **434**, 67–76 (2011).
41. Matz, M. V., Treml, E. A. & Haller, B. C. Estimating the potential for coral adaptation to global warming across the Indo-West Pacific. *Glob. Change Biol.* **26**, 3473–3481 (2020).
42. McManus, L. C. et al. Evolution and connectivity influence the persistence and recovery of coral reefs under climate change in the Caribbean, Southwest Pacific, and Coral Triangle. *Glob. Change Biol.* **27**, 4307–4321 (2021).
43. Cheung, M. W., Hock, K., Skirving, W. & Mumby, P. J. Cumulative bleaching undermines systemic resilience of the Great Barrier Reef. *Curr. Biol.* **31**, 5385–5392. e4 (2021).

44. McWhorter, J. K., Halloran, P. R., Roff, G., Skirving, W. J. & Mumby, P. J. Climate refugia on the Great Barrier Reef fail when global warming exceeds 3°C. *Glob. Change Biol.* **28**, 5768–5780 (2022).
45. Sun, C. et al. Climate refugia in the Great Barrier Reef may endure into the future. *Sci. Adv.* **10**, eado6884 (2024).
46. Cresswell, A. K. et al. Capturing fine-scale coral dynamics with a metacommunity modelling framework. *Sci. Rep.* **14**, 24733 (2024).
47. Selmoni, O., Lecellier, G., Vigliola, L., Berteaux-Lecellier, V. & Joost, S. Coral cover surveys corroborate predictions on reef adaptive potential to thermal stress. *Sci. Rep.* **10**, 19680 (2020).
48. McManus, L. C. et al. Evolution reverses the effect of network structure on metapopulation persistence. *Ecology* **102**, e03381 (2021).
49. Oliver, J. & Babcock, R. Aspects of the fertilization ecology of broadcast spawning corals: sperm dilution effects and in situ measurements of fertilization. *Biol. Bull.* **183**, 409–417 (1992).
50. van Oppen, M. J. & Gates, R. D. Conservation genetics and the resilience of reef-building corals. *Mol. Ecol.* **15**, 3863–3883 (2006).
51. Urban, M. C. et al. When and how can we predict adaptive responses to climate change?. *Evol. Lett.* **8**, 172–187 (2024).
52. Roik, A. et al. Trade-offs in a reef-building coral after six years of thermal acclimation. *Sci. Total Environ.* **949**, 174589 (2024).
53. Cornwell, B. et al. Widespread variation in heat tolerance and symbiont load are associated with growth tradeoffs in the coral Acropora hyacinthus in Palau. *Elife* **10**, e64790 (2021).
54. Howells, E. J. et al. Coral thermal tolerance shaped by local adaptation of photosymbionts. *Nat. Clim. Change* **2**, 116–120 (2012).
55. Anthony, K. R. et al. Interventions to help coral reefs under global change—a complex decision challenge. *PLoS ONE* **15**, e0236399 (2020).
56. Mumby, P. J. et al. Reserve design for uncertain responses of coral reefs to climate change. *Ecol. Lett.* **14**, 132–140 (2011).
57. Colton, M. A. et al. Coral conservation in a warming world must harness evolutionary adaptation. *Nat. Ecol. Evol.* **6**, 1405–1407 (2022).
58. Walsworth, T. E. et al. Management for network diversity speeds evolutionary adaptation to climate change. *Nat. Clim. Change* **9**, 632–636 (2019).
59. Kleypas, J. A. et al. Larval connectivity across temperature gradients and its potential effect on heat tolerance in coral populations. *Glob. Change Biol.* **22**, 3539–3549 (2016).
60. Castro-Sanguino, C. et al. Control efforts of crown-of-thorns starfish outbreaks to limit future coral decline across the Great Barrier Reef. *Ecosphere* **14**, e4580 (2023).
61. Mason, R. A., Bozec, Y.-M. & Mumby, P. J. Demographic resilience may sustain significant coral populations in a 2 °C-warmer world. *Glob. Change Biol.* **29**, 4152–4160 (2023).
62. Mason, R. A., Bozec, Y.-M. & Mumby, P. J. Setting sustainable limits on anchoring to improve the resilience of coral reefs. *Mar. Pollut. Bull.* **189**, 114721 (2023).
63. Roelfsema, C. M. et al. How much shallow coral habitat is there on the Great Barrier Reef?. *Remote Sens.* **13**, 4343 (2021).
64. Hock, K. et al. Connectivity and systemic resilience of the Great Barrier Reef. *PLoS Biol.* **15**, e2003355 (2017).
65. Carrigan, A. D. & Puotinen, M. Tropical cyclone cooling combats region-wide coral bleaching. *Glob. Change Biol.* **20**, 1604–1613 (2014).
66. Baird, A. H. et al. A decline in bleaching suggests that depth can provide a refuge from global warming in most coral taxa. *Mar. Ecol. Prog. Ser.* **603**, 257–264 (2018).
67. Naugle, M. S. et al. Heat tolerance varies considerably within a reef-building coral species on the Great Barrier Reef. *Commun. Earth Environ.* **5**, 525 (2024).
68. Marzonie, M. R. et al. The effects of marine heatwaves on acute heat tolerance in corals. *Glob. Change Biol.* **29**, 404–416 (2023).
69. Visscher, P. M., Hill, W. G. & Wray, N. R. Heritability in the genomics era-concepts and misconceptions. *Nat. Rev. Genet.* **9**, 255–266 (2008).
70. Angilletta, M. J. *Thermal Adaptation: A Theoretical and Empirical Synthesis* (Oxford University Press, 2009).
71. Falconer, D. & Mackay, F. *Introduction to Quantitative Genetics* (Longman, 1996).
72. Lynch, M. & Walsh, B. *Genetics and Analysis of Quantitative Traits*, Vol. 1 (Sinauer Sunderland, 1998).
73. Bozec, Y.-M. & Mumby, P. J. Detailed description of ReefMod-GBR and simulation results. Technical Appendix B2. in *Reef Restoration and Adaptation Program: Modelling Methods and Findings. A Report Provided to the Australian Government by the Reef Restoration and Adaptation Program* (eds Anthony, K. R. N. et al.) 72–113 (Australian Institute of Marine Science, 2019).
74. Hock, K., Doropoulos, C., Gorton, R., Condie, S. A. & Mumby, P. J. Split spawning increases robustness of coral larval supply and inter-reef connectivity. *Nat. Commun.* **10**, 3463 (2019).
75. Herzfeld, M. et al. *eReefs Marine Modelling: Final Report*. 497 http://www.marine.csiro.au/cem/gbr4/eReefs_Marine_Modelling.pdf (2016).
76. Bureau of Meteorology. Australian Tropical Cyclone Database. http://www.bom.gov.au/cyclone/tropical-cyclone-knowledge-centre/databases/ (Accessed 07 Feb 2024).
77. Baird, M. E. et al. CSIRO Environmental Modelling Suite (EMS): scientific description of the optical and biogeochemical models (vB3p0). *Geosci. Model Dev.* **13**, 4503–4553 (2020).
78. Halloran, P. R., McWhorter, J. K., Arellano Nava, B., Marsh, R. & Skirving, W. S. 2P3-R v2. 0: computationally efficient modelling of shelf seas on regional to global scales. *Geosci. Model Dev.* **14**, 6177–6195 (2021).
79. Wolff, N. H. et al. Temporal clustering of tropical cyclones on the Great Barrier Reef and its ecological importance. *Coral Reefs* **35**, 613–623 (2016).
80. Knutti, R., Rugenstein, M. A. & Hegerl, G. C. Beyond equilibrium climate sensitivity. *Nat. Geosci.* **10**, 727–736 (2017).
81. Forster, P. et al. The Earth's energy budget, climate feedbacks, and climate sensitivity. in *Climate Change 2021: The Physical Science Basis. Contribution of Working Group I to the Sixth Assessment Report of the Intergovernmental Panel on Climate Change* 923–1054 (Cambridge University Press, 2021).
82. Sherwood, S. C. et al. An assessment of Earth's climate sensitivity using multiple lines of evidence. *Rev. Geophys.* **58**, e2019RG000678 (2020).
83. Pinheiro, J. C. & Bates, D. M. Linear mixed-effects models: basic concepts and examples. *Mix. Eff. Models* **3**, 56 (2000).
84. Jaeger, B. C., Edwards, L. J., Das, K. & Sen, P. K. An R^2 statistic for fixed effects in the generalized linear mixed model. *J. Appl. Stat.* **44**, 1086–1105 (2017).
85. Bozec, Y.-M. GBR.7.0_Futures_CMIP6: ReefMod-GBR forecast analyses (Version 1). Zenodo. https://doi.org/10.5281/zenodo.17158652 (2025).
86. Bozec, Y.-M. ReefMod-GBR version 7.0. Zenodo. https://doi.org/10.5281/zenodo.16734996 (2025).

Acknowledgements

We acknowledge the Traditional Owners of the Great Barrier Reef, and pay our respects to their Elders past, present, and emerging and recognise their continuing spiritual connection to sea country. This work was funded by the Reef Restoration and Adaptation Program, a partnership between the Australian Government's Reef Trust and the Great Barrier Reef Foundation. We thank D. Mead, C. Robillot, M. Baskett, C.

Kenkel, A. Baker, K. McGuigan and C. Castro-Sanguino for insightful comments at various stages of this work. We thank J.T. Morris from NOAA for a thoughtful review of the manuscript. J. Gilmour, M. Gonzalez-Rivero, D. Barneche, B. Robson and J. Moore contributed to the development of the model C~scape, and R. Ferrari, C. Doropoulos, M. Toor, S. Gordon, K. Crossman and M. Puotinen contributed to its parameterisation.

Author contributions

Y.-M.B. and P.J.M. conceived the study, performed the analysis and wrote the first draft of the manuscript. Y.-M.B. designed and implemented the model ReefMod. J.K.M., B.A.N. and P.R.H. downscaled the warming projections. A.K.C., V.H.-B. and J.-C.O. designed and implemented the model C~scape. A.A.S.A., T.I., L.L., S.A.M., K.R.N.A., S.A.C. and C.R. provided comments on the results. All authors contributed to writing the final manuscript.

Competing interests

The authors declare no competing interests.

Additional information

Supplementary information The online version contains supplementary material available at https://doi.org/10.1038/s41467-025-65015-4.

Correspondence and requests for materials should be addressed to Yves-Marie Bozec.

Peer review information *Nature Communications* thanks Raúl González-Pech and the other, anonymous, reviewer(s) for their contribution to the peer review of this work. A peer review file is available.

Reprints and permissions information is available at http://www.nature.com/reprints

Publisher's note Springer Nature remains neutral with regard to jurisdictional claims in published maps and institutional affiliations.

Open Access This article is licensed under a Creative Commons Attribution-NonCommercial-NoDerivatives 4.0 International License, which permits any non-commercial use, sharing, distribution and reproduction in any medium or format, as long as you give appropriate credit to the original author(s) and the source, provide a link to the Creative Commons licence, and indicate if you modified the licensed material. You do not have permission under this licence to share adapted material derived from this article or parts of it. The images or other third party material in this article are included in the article's Creative Commons licence, unless indicated otherwise in a credit line to the material. If material is not included in the article's Creative Commons licence and your intended use is not permitted by statutory regulation or exceeds the permitted use, you will need to obtain permission directly from the copyright holder. To view a copy of this licence, visit http://creativecommons.org/licenses/by-nc-nd/4.0/.

© The Author(s) 2025